Pergamon

Journal of Terramechanics, Vol. 33, No. 4, pp. 185–194, 1996
Published by Elsevier Science Ltd on behalf of ISTVS
Printed in Great Britain
0022–4898/96 $15.00+0.00

PII: S0022–4898(97)00003–7

SOIL STRESS STATE ORIENTATION BENEATH A TIRE AT VARIOUS LOADS AND INFLATION PRESSURES

T. R. WAY,* C .E. JOHNSON,† A. C. BAILEY,* R. L. RAPER* and E. C. BURT*

Summary—Stress state transducers (SSTs) were used to determine the orientation of the major principal stress, σ_1, in soil beneath the centerline of an 18.4R38 radial-ply R-1 drive tire operated at 10% slip. Two soils, a sandy loam and a clay loam, were each prepared twice to obtain two density profiles. One profile of each soil had a hardpan and the soil above the hardpan was loose. The soil in the second profile was loosely tilled. The stress state was determined at a depth of 358 mm in the sandy loam and 241 mm in the clay loam soil. The tire was operated at two dynamic loads (13.2 and 25.3 kN), each at two levels of inflation pressure (41 and 124 kPa). When the orientation of σ_1 was determined directly beneath the axle, the mean angles of tilt in the direction of travel ranged from 6 to 23 degrees from vertical. Inflation pressure did not significantly affect the angle when the dynamic load was 13.2 kN in the sandy loam soil, and neither inflation pressure nor dynamic load significantly affected the angle in the clay loam soil. When the dynamic load was 25.3 kN in the sandy loam soil, the orientation of the major principal stress determined directly beneath the axle was tilted significantly more in the direction of travel when the tire was at 41 kPa inflation pressure than when at 124 kPa. These changes in stress orientation demonstrate the importance of measuring the complete stress state in soil, rather than stresses along only one line of action. The changing orientation of σ_1 as the tire passes over the soil indicates the soil undergoes kneading and supports future investigation of the contribution of changes in stress orientation to soil compaction. Published by Elsevier Science Ltd on behalf of ISTVS.

INTRODUCTION

The stress state in soil beneath drive tires has been determined using stress state transducers (SSTs) for various conditions. The primary objective of stress measurement in soil has been to relate the stresses to soil compaction caused by the stresses. Soil stresses determined beneath the centerline and edge of the tread of a radial-ply tractor tire, operated at one dynamic load at each of four inflation pressures, showed that the mean of the peak major principal normal stress, σ_1, exceeded the mean of the normal stress measured in the vertical direction at each inflation pressure in both a sandy loam and a clay loam soil [1]. Therefore, the orientation of σ_1 was usually not vertical at the location where σ_1 was maximum.

The orientation of the major principal stress in Norfolk sandy loam soil beneath the centerline of an 18.4–38 bias-ply tire was shown by Bailey *et al.* [2] to sweep through an

*Agricultural Engineers, USDA, ARS, National Soil Dynamics Laboratory, P.O. Box 3439, Auburn, Alabama 36831-3439, U.S.A.
†Professor, Alabama Agricultural Experiment Station, Agricultural Engineering Department, Auburn University, Alabama 36849-5417, U.S.A.

angle of approximately 90 degrees as the tire passed over the SST. Orientation of the major principal stress in soil beneath a rigid wheel was shown by Karafiath and Nowatzki [3] to generally tilt rearward from vertical in the forward failure zone and tilt forward in the rearward failure zone.

Effects of inflation pressure and dynamic load on the orientation of stresses in soil beneath tractor tires are not well established. Changes in the orientation of σ_1 as the stress is applied may affect the soil compaction caused by a given stress magnitude [4]. If the orientation of σ_1 changes, the importance of measuring the complete stress state, rather than stresses along only one line of action, increases. Therefore, an experiment was developed with an objective of determining the effect of dynamic load and inflation pressure of a radial-ply drive tire on the orientation of the major principal normal stress in soil beneath the tire. Analyses of soil stress magnitudes and soil bulk density measured in this experiment were reported by Bailey *et al.* [5] and analyses of soil-tire interface pressures, rut width and rut cross-sectional area were reported by Raper *et al.* [6].

PROCEDURES

The experiment was conducted in the soil bins at the National Soil Dynamics Laboratory (NSDL), a facility of the USDA Agricultural Research Service in Auburn, Alabama, U.S.A., using the NSDL single wheel traction research vehicle [7] and the NSDL data acquisition and control system [8]. A new 18.4R38 Goodyear* Dyna Torque Radial (2-Star) R-1 tire was operated by the traction research vehicle.

The experiment was conducted on the NSDL's two indoor soil bins, one containing Norfolk sandy loam soil (*Typic Paleudults*) and the other containing Decatur clay loam soil (*Rhodic Paleudults*). The composition of the sandy loam was 71.6% sand, 17.4% silt and 11.0% clay, and the composition of the clay loam was 26.9% sand, 43.4% silt and 29.7% clay. Each soil bin was prepared twice to obtain two different density profiles. A hardpan profile was established in each soil by first rotary tilling the soil to a depth of about 600 mm. The hardpan was formed across the whole area of each bin by using side-by-side passes of a single moldboard plow followed by a steel wheel operating in the plow furrow. The loose soil above the hardpan was leveled with a scraper blade after the hardpan was formed. The top of the hardpan was 410 mm beneath the loose surface of the sandy loam and 300 mm beneath the loose surface of the clay loam. The second profile of each soil was a uniform profile and was formed by rotary tilling to a depth of about 600 mm and then leveling the surface of the soil with a scraper blade. Initial conditions of the soils are given in Table 1. The soil moisture contents and bulk densities were determined gravimetrically using cylindrical soil samples 40 mm in height and 69 mm in diameter.

An SST was used to determine stresses in the soil beneath the tire. The SST consisted of pressure sensors with diaphragm diameters of 9.7 mm, similar to the SST described by Nichols *et al.* [9] (Fig. 1). The SST measured six soil pressures which were used to calculate the complete stress state of the soil at the transducer. The orientations of three of the SST pressure sensor diaphragms, designated x, y and z, are normal to the x, y and z axes

*Tire provided by The Goodyear Tire and Rubber Company. Mention of trademarks or company names does not imply endorsement of these products by the USDA or Auburn University.

of a right-handed coordinate system. The stress state is a 3 × 3 real symmetric matrix which has three eigenvalues and three eigenvectors. The eigenvalues are the magnitudes of the principal stresses: σ_1, σ_2 and σ_3. Each eigenvector consists of three direction cosines, which are the cosines of the included angles between the line of action of the principal stress and the x, y and z axes of the SST.

The treatments in the experiment were different combinations of dynamic load and inflation pressure (Table 2). The 13.2-41 and 25.3-124 treatments are two combinations recommended by the tire manufacturer [10], so the tire had the recommended inflation pressure for each dynamic load. The 13.2-124 treatment over-inflated the tire because the 124 kPa inflation pressure was greater than the 41 kPa recommended for a 13.2 kN dynamic load. Farmers have commonly used over-inflated radial-ply tractor tires because the tires are often inflated until there is little or no sidewall bulge, so they look like bias-ply tires [11].

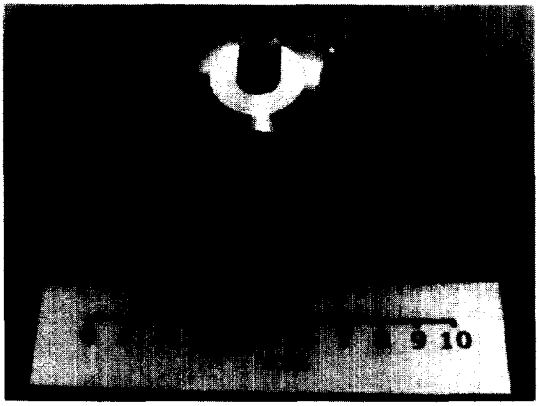

Fig. 1. Stress state transducer (SST).

Table 1. Mean initial conditions of soils

Soil	Profile	In loose soil from 10 to 50 mm above the hardpan or at same depth in the uniform profile: Moisture content (% d.b.)	Bulk density (Mg/m^3)	Cone index (MPa)	In hardpan (10 to 50 mm beneath top of hardpan: Bulk density (Mg/m^3)	Cone index (MPa)
Sandy loam	Uniform	7.6	1.19	0.94		
Sandy loam	Hardpan	7.1	1.32	0.72	1.89	6.03
Clay loam	Uniform	13.4	1.08	1.26		
Clay loam	Hardpan	12.9	1.10	0.98	1.81	3.82

Note:
Cone penetrometer and procedure are described in [12].
Base area of cone penetrometer = 323 mm^2.

Table 2. Dynamic load and inflation pressure combinations

Treatment	Dynamic load (kN)	Inflation pressure (kPa)
13.2-41	13.2	41
13.2-124	13.2	124
25.3-41	25.3	41
25.3-124	25.3	124

The 25.3-41 treatment under-inflated the tire and is not recommended by the manufacturer for field use.

For all tests, the forward velocity of the tire was 0.15 m/s and slip was 10%. Zero conditions for slip calculations consisted of the tire operating on concrete at zero net traction. The traction research vehicle was controlled by computer throughout each test. For each combination of soil and profile, the soil bin was divided into four blocks (replications), each consisting of four plots, one per test. The dynamic load and inflation pressure treatments were randomly assigned to the plots in each block. In each plot, the SST was buried in the soil beneath the centerline of the tire path to be trafficked, and the tire was then operated on the soil. In the hardpan profile of each soil, the SST rested on the hardpan and the same initial SST depth was used in the uniform profile. The mean initial depth of the top of the SST beneath the loose soil surface, averaged across both soil profiles, was 358 mm in the sandy loam and 241 mm in the clay loam.

RESULTS

The pressures applied to the sensors on the SST were designated p_x, p_y, p_z, p_1, p_2 and p_3. The SST was buried with the p_z diaphragm facing up and the tire direction of travel bisecting normals to the p_x and p_y diaphragms (Fig. 2). Normals to the p_1, p_2 and p_3 diaphragms were each tilted 54.7 degrees downward from vertical. An example of pressure data sensed by the six individual pressure sensors of the SST during a tire pass is shown in Fig. 3. The data were actually collected while the SST was buried in the soil, with the tire passing over the SST, but the data in Fig. 3 have been transformed to show pressure measurements forward and rearward of the axle. The value of 0 on the distance axis represents the longitudinal position of the wheel axle. Data at positive distance values represent pressures in front of the axle and data at negative distances represent pressures to the rear of the axle.

The calculated principal stresses (σ_1, σ_2 and σ_3) and the octahedral stresses (σ_{oct} and τ_{oct}) for the data in Fig. 3 are shown in Fig. 4 using the same distance axis used in Fig. 3. Direction cosines for σ_1 relative to the x, y and z axes of the SST show that the orientation of σ_1 was nearly vertical approximately 0.1 m in front of the axle (Fig. 5). At other positions, the orientation of σ_1 was not vertical, as evidenced by direction cosines with

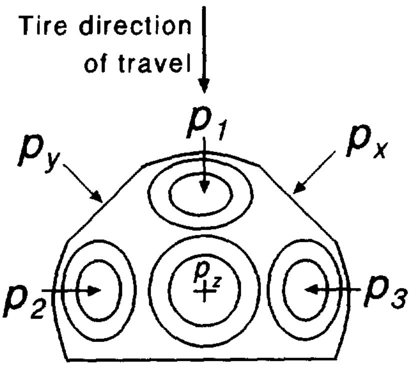

Fig. 2. Top view of stress state transducer as it was placed in the soil.

respect to the z axis being less than 1. Direction cosines determined outside of the distance range from −0.3 m to 0.5 m are considered to be unreliable due to the small magnitude of σ_1 (Fig. 4).

Orientations of σ_1 applied to soil elements at four locations under the tire, just above the hardpan, for four combinations of dynamic load and inflation pressure are shown for the sandy loam in Fig. 6, and for the clay loam in Fig. 7. The point of each σ_1, shown in the side views of Figs 6 and 7, corresponds to the location of the stress relative to the axle, and each σ_1 orientation and magnitude represents the mean of four replications. In the hardpan profiles, the initial depth of the top of the SST beneath the loose soil surface was

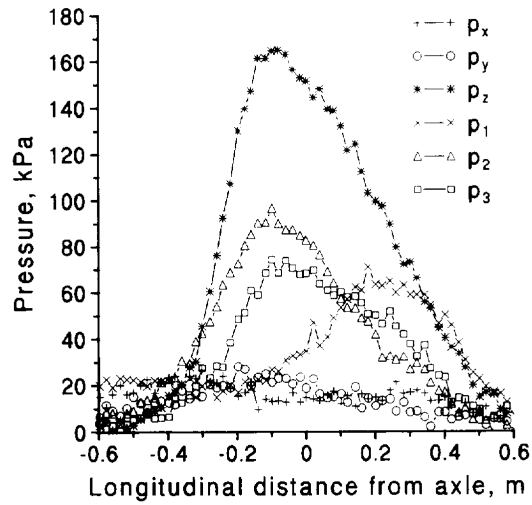

Fig. 3. Pressures measured by an SST in the sandy loam soil with the hardpan profile beneath the centerline of the tire with inflation pressure = 124 kPa and dynamic load = 25.3 kN.

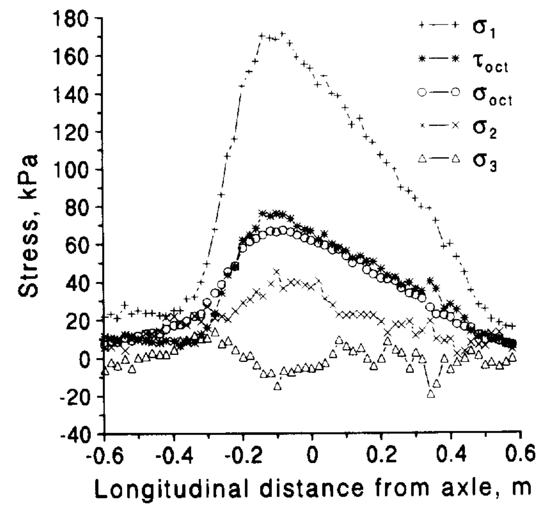

Fig. 4. Calculated stresses from data shown in Fig. 3.

357 mm in the sandy loam and 238 mm in the clay loam. Figures 6 and 7 are shown to scale, but the relationship between the stress and length scales is arbitrary. In the side views in Figs 6 and 7, the tire shape is shown as a circle and does not account for the true tire carcass deflection. Rut depths were determined using a 215 mm diameter wheel rolling

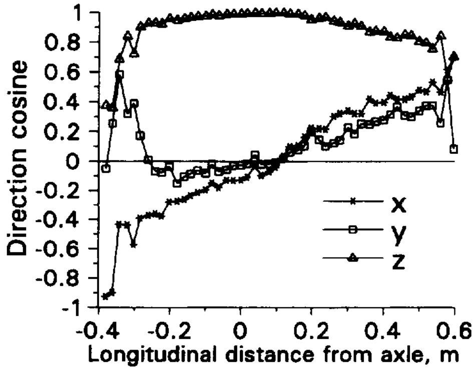

Fig. 5. Direction cosines of σ_1 with respect to the SST x, y and z axes for the data shown in Figs 3 and 4.

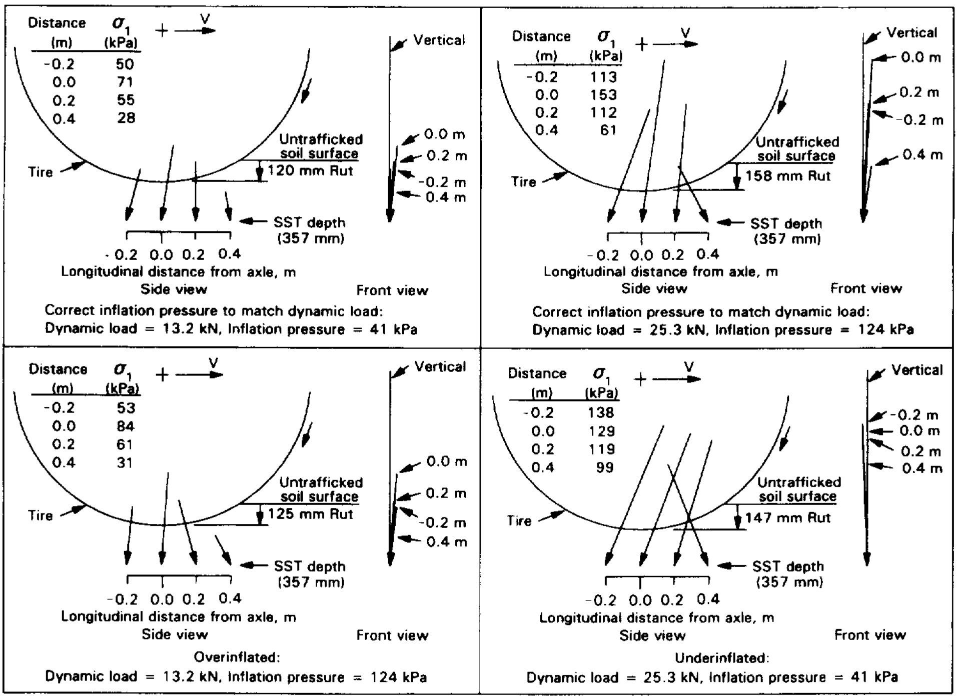

Fig. 6. Stresses in the hardpan profile of the sandy loam soil. Side and front views of σ_1 applied at four positions beneath the centerline of the tire path for four combinations of dynamic load and inflation pressure with the Stress State Transducer (SST) resting on the hardpan. Initial depth of top of SST was 357 mm beneath untrafficked soil surface. The point of each σ_1 represents the stress location relative to the tire. Each σ_1 represents the mean orientation and magnitude of four replications. Line designated "Vertical" in front views is the central plane of the tire.

on the centerline of the rut, so the rut depths are approximately the depths of the tire undertread imprints. The tire lug height at the tread centerline was 41 mm. In the clay loam, the result showing the mean rut depth of 128 mm in the 25.3-41 treatment as slightly greater than the 124 mm rut depth in the 25.3-124 treatment was unexpected. The two means were compared using a *t*-test, however, and were not significantly different at the 5% significance level.

Within each combination of dynamic load and inflation pressure, differences in the trend of the σ_1 orientations shown in Figs 6 and 7 may have resulted from the soil type, the depth of stress measurement, or both. The front views in Figs 6 and 7 show that the σ_1 orientations deviated slightly from the central plane of the tire in the sandy loam, and to a greater extent in the clay loam. These deviations likely resulted from non-uniformities in the soils, particularly the aggregates in the clay loam.

The angle between the projection of σ_1 on the vertical-longitudinal plane and a vertical line was calculated at two locations in each data set:

1. directly beneath the axle (longitudinal distance = 0),
2. where the magnitude of σ_1 was maximum.

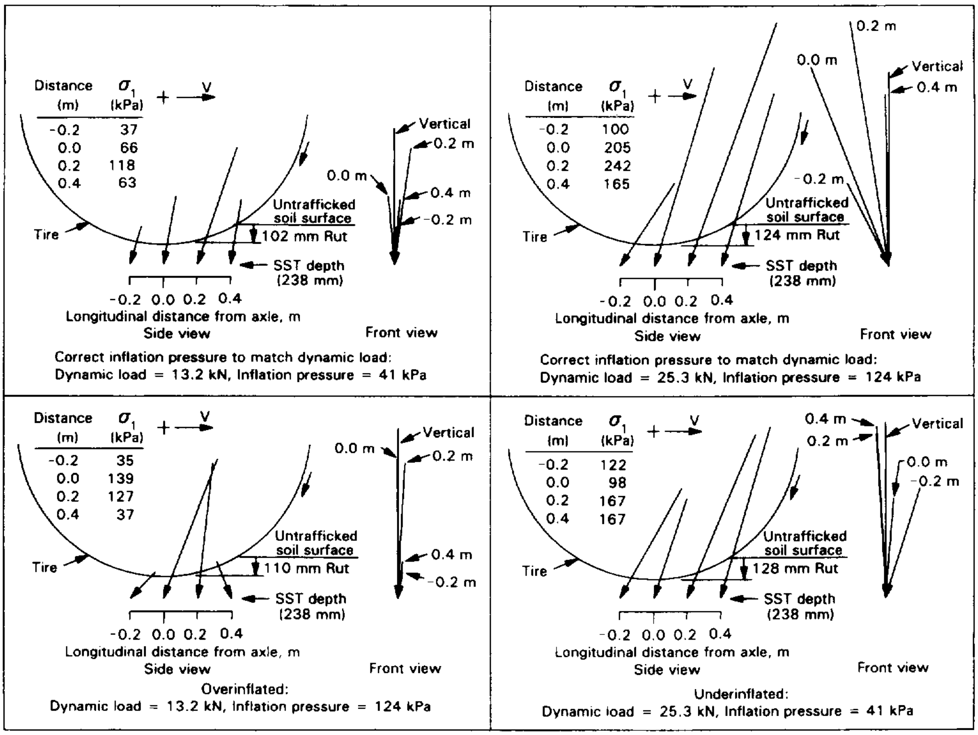

Fig. 7. Stresses in the hardpan profile of the clay loam soil. Side and front views of σ_1 applied at four positions beneath the centerline of the tire path for four combinations of dynamic load and inflation pressure with the Stress State Transducer (SST) resting on the hardpan. Initial depth of top of SST was 238 mm beneath untrafficked soil surface. The point of each σ_1 represents the stress location relative to the tire. Each σ_1 represents the mean orientation and magnitude of four replications. Line designated "Vertical" in front views is the central plane of the tire.

An angle of zero means the projection of σ_1 on the vertical-longitudinal plane was vertical and a positive angle means the projection was tilted in the direction of travel (Fig. 8). For both angles, all means were positive when averaged over the four replications (Table 3). The result showing that the angles were positive directly beneath the axle was expected because the geometric center of the tire footprint was typically forward of the axle [6] and the tire had a positive net traction throughout the experiment resulting from the controlled slip value of 10%.

Analyses of variance were used to determine the effect of dynamic load and inflation pressure on the two angles. A separate analysis of variance was conducted for each soil type because the initial depth of the SST differed for the two soils. Within each soil type, replication was nested within the soil profile. SAS programs were used to evaluate the effect of dynamic load and inflation pressure, and their interactions, on the two angles (SAS Institute, Inc., Cary, NC). The main effects of dynamic load and inflation pressure did not significantly affect either angle at the 5% level. In the sandy loam, the interaction of dynamic load and inflation pressure significantly affected the angle determined directly beneath the axle ($p = 0.0271$). Therefore, two more analyses of variance were conducted for the sandy loam, one for each level of dynamic load. The analysis for the 13.2 kN dynamic load showed that the angle determined directly beneath the axle was not significantly affected by inflation pressure ($p = 0.0915$). The analysis for the 25.3 kN load, however, showed that the mean angle of 21.7 degrees for the 41 kPa inflation pressure was significantly greater than the mean angle of 7.8 degrees for the 124 kPa inflation pressure

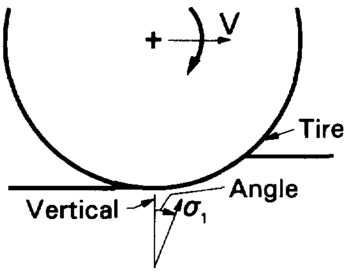

Fig. 8. Positive angle between projection of σ_1 onto vertical-longitudinal plane and vertical.

Table 3. Mean angles between the projection of σ_1 on the vertical-longitudinal plane, and a vertical line at two locations: (1) directly beneath the axle, and (2) where the magnitude of σ_1 was maximum

			Norfolk sandy loam		Decatur clay loam	
Profile	Dynamic load (kN)	Inflation pressure (kPa)	Angle at axle (deg)	Angle at maximum σ_1 (deg)	Angle at axle (deg)	Angle at maximum σ_1 (deg)
Hardpan	13.2	41	10.3	15.2	8.2	23.3
Hardpan	13.2	124	6.8	3.5	19.4	9.5
Hardpan	25.3	41	20.6	6.4	17.6	24.1
Hardpan	25.3	124	9.3	16.9	12.2	22.9
Uniform	13.2	41	6.3	9.2	12.7	23.7
Uniform	13.2	124	19.5	21.1	21.1	26.5
Uniform	25.3	41	22.8	26.7	21.5	36.9
Uniform	25.3	124	6.2	8.0	18.2	19.4

Angles are zero when the projected orientation is vertical, and positive when tilted in the direction of travel.

($p = 0.0430$). The significantly greater angle for the 41 kPa inflation pressure likely resulted from the fact that the length of the tire footprint extending forward from the axle was greater for the 41 kPa inflation pressure [6], so the geometric center of the footprint was farther forward of the axle than it was for the 124 kPa inflation pressure.

The orientation of σ_1 determined at a fixed location in the soil changes as the tire passes over the soil, as shown by the direction cosines in Fig. 5. One measure of these changes in orientation is the change in angle, in three-dimensional space, between the orientation of σ_1 at one location and at the next measurement location. The longitudinal distance between consecutive measurement locations used by the data acquisition system in this experiment was 20 mm. The change in orientation between consecutive positions was calculated using a vector scalar product (dot product) to determine the included angle between a vector along the line of action of σ_1 at one location and at the next location, 20 mm away. The change in angle between consecutive σ_1 orientations for the data set shown in Figs 3–5 attained its minimum of 0.33 degrees at a position 0.08 m to the rear of the axle (Fig. 9). The change in angle was rapid for locations from +0.4 to +0.5 m and from −0.2 to −0.3 m. The changes in angle determined outside of the distance range from −0.3 m to 0.5 m are considered to be unreliable due to the small magnitude of σ_1.

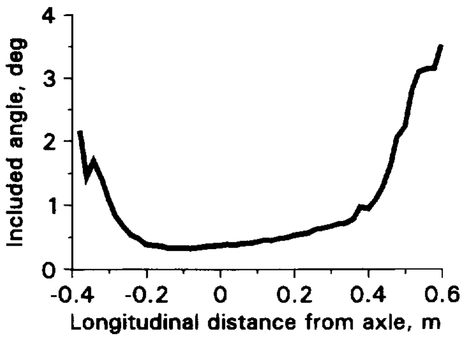

Fig. 9. Change in angle, in three-dimensional space, between consecutive σ_1's when the longitudinal diatance between measurements was 20 mm.

In summary, this experiment shows that the orientation of σ_1 in soil beneath a tractor drive tire operating at 10% slip depends on the longitudinal distance of the stress from the axle, and is typically not vertical. These changes in stress orientation demonstrate the importance of measuring the complete stress state rather than stresses along only one line of action. The changing orientation of σ_1 as the tire passes over the soil indicates the soil undergoes kneading. These results support the need for future investigation of the contribution of changes in stress orientation, in addition to stress magnitude, to soil compaction.

CONCLUSIONS

The orientation of the major principal stress determined directly beneath the axle of a radial-ply drive tire, operating at 10% slip with a dynamic load of 25.3 kN on a sandy loam soil, was tilted significantly more in the direction of travel when the inflation pressure was 41 kPa than when it was 124 kPa, when the stress state was determined at a depth of 358 mm. Inflation pressure did not significantly affect the angle when the dynamic load was 13.2 kN in the sandy loam soil when the stress state was determined at a depth of 358 mm, and neither inflation pressure nor dynamic load significantly affected the angle in a clay loam soil when the stress state was determined at a depth of 241 mm.

Acknowledgements—The authors acknowledge technical contributions of Deere and Company and The Goodyear Tire & Rubber Company.

REFERENCES

1. Bailey, A. C., Raper, R. L. and Burt, E. C. The effects of tire inflation pressure on soil stresses. ASAE paper no. 911062, ASAE, 1991. St. Joseph, Michigan, USA.
2. Bailey, A. C., Nichols, T. A. and Johnson, C. E., Soil stress state determination under wheel loads. *Transactions of the. ASAE*, 1988, **31**(5), 1309–1314.
3. Karafiath, L. L. and Nowatzki, E. A., *Soil mechanics for off-road vehicle engineering*. Trans Tech Publications. Clausthal, Germany, p. 125.
4. Koolen, A. J. and Kuipers, H., *Agricultural Soil Mechanics*. Springer-Verlag, Berlin, 1983, p. 31.
5. Bailey, A. C., Raper, R. L., Way, T. R., Burt, E. C. and Johnson, C. E. Soil stresses under a tractor tire at various loads and inflation pressures. *Journal of Terramechanics*, 1996, **33**(1), 1–11.
6. Raper, R. L., Bailey, A. C., Burt, E. C., Way, T. R. and Liberati, P. Inflation pressure and dynamic load effects on soil deformation and soil-tire interface stresses. *Transactions of the ASAE*, 1989, **38**(3), 685–689 .
7. Burt, E. C., Reaves, C. A., Bailey, A. C. and Pickering, W. D. A machine for testing tractor tires in soil bins. *Transactions of the ASAE*, 1980, **23**(3), 546–547, 552.
8. Lyne, P. W. L., Burt, E. C. and Jarrell, J. D., Computer control for the NTML single-wheel tester. ASAE paper no. 83-1555, ASAE, St. Joseph, Michigan, USA 1983.
9. Nichols, T. A., Bailey, A. C., Johnson, C. E. and Grisso, R. D. A stress state transducer for soil. *Transactions of the ASAE*, 1987, **30**(5), 1237–1241.
10. Goodyear, *Optimum Tractor Tire Performance Handbook*. The Goodyear Tire and Rubber Company, Akron, Ohio, USA 1992.
11. Wiley, J. C., Romig, B. E., Anderson, L. V. and Zoz, F. M., Optimizing dynamic stability and performance of tractors with radial tires. ASAE paper no. 921586, ASAE, St. Joseph, Michigan, USA 1992.
12. ASAE, *ASAE Standards*. 42nd ed. S313.2. Soil Cone Penetrometer. ASAE, St. Joseph, Michigan, USA 1995.